Hindawi
Advances in Civil Engineering
Volume 2020, Article ID 8219712, 12 pages
https://doi.org/10.1155/2020/8219712

Research Article

Experimental Investigation of Progressive Collapse of Prestressed Concrete Frames after the Loss of Middle Column

Tao Yang,[1,2,3] **Wanqing Chen**,[1] **and Zhongqing Han**[1]

[1]*College of Civil Engineering and Architecture, Guangxi University, Nanning 530004, China*
[2]*Guangxi Key Laboratory of Disaster Prevention and Engineering Safety, Nanning 530004, China*
[3]*Key Laboratory of Disaster Prevention and Structural Safety of Ministry of Education, Nanning 530004, China*

Correspondence should be addressed to Tao Yang; yt48440002@163.com

Received 6 August 2019; Revised 18 December 2019; Accepted 31 January 2020; Published 26 February 2020

Academic Editor: Zaobao Liu

Accidental loads such as explosion and vehicle impact could lead to failure of one or several load-bearing members in the structures, which is likely to trigger disproportionate progressive collapse of overall structures. Prestressed concrete (PC) frame structures are usually at great risk of collapse once load-bearing members fail, because the members in PC frame structures are usually subjected to much more load than those in common reinforced concrete (RC) frame structures. To investigate the progressive collapse behaviors of PC frame structures, five one-fourth reduced scaled frame substructures were fabricated and collapse tests were conducted on them. Influence of span-to-depth ratios of frame beams and prestress action modes on the collapse performance of PC frame structures was discussed. Experimental results indicated that PC frame substructures with different prestress action modes, including bonded prestress and unbonded prestress, presented different collapse resistance capabilities and deformability. Tensile force increment of the unbonded prestressing strands almost linearly increased with the vertical displacement of the failed middle column. Catenary action is one of the most important mechanisms in resisting structural collapse. Prestressing strands and longitudinal reinforcing bars in the frame beams benefited the formation and maintaining of catenary action. The ultimate deformability of the PC frame structures was tightly connected with the fracture of prestressing strand. In addition, a calculation method of dynamic increase factors (DIFs) suitable for PC frame structures was developed, which can be used to revise the design collapse load when static collapse analysis is conducted by the alternative path method. The DIFs of the five substructures were discussed on the basis of the proposed method; it revealed that the DIFs corresponding to the first peak loads and the ultimate failure loads for the PC frame substructures were less than 1.49 and 1.83, respectively.

1. Introduction

Load-bearing members in frame structures might fail under accidental loads such as explosion, vehicle impact, and so on, which can trigger disproportional collapse of integral structures. In the past several decades, many disastrous structural collapse accidents had occurred, such as collapse of the Ronan Point apartment in Britain in 1986 due to fire and the Alfred P. Murrah federal building in America in 1995 due to terrorist attack. Therefore, researchers all over the world paid much attention to progressive collapse of structures over the years that followed. As reinforced concrete (RC) frame structures are widely used in industrial and civil buildings, many research works have been conducted to investigate their collapse mechanisms. Compressive arch action and catenary action formed in frame beams during structural collapse had been experimentally proved to be effective to improve the collapse resistance of RC frame structures [1–3]. Due to limitation of lab conditions, most collapse tests on RC frame structures in labs adopted frame models without floor slabs. As a result, some researchers investigated the influence of slabs on structural collapse performance by tests or numerical analysis [4, 5], and it was found that slab could significantly improve the resistance capability against collapse after the failure of load-bearing columns. In fact, collapse process of structures is dynamic and their collapse behaviors are apparently different from those revealed by static collapse tests. Some design

parameters such as design span length of frame beams can greatly affect the dynamic responses of frame structures during collapse [6]. To obtain the actual collapse responses of RC frame structures, Sasani and Sagiroglu [7, 8] conducted on-site demolition tests on an abandoned building, and Vierendeel action was identified as the major mechanism for load redistribution in the residual structures. Furthermore, different assessment methods were established to assess the inherent collapse resistance of RC frame structures [9–11]. In recent years, progressive collapse performance of precast concrete frames has been investigated because of their increasing application, and improved beam-column connection details and constructional measures were proposed to mitigate collapse risk of precast concrete frames [12–14].

When RC frame structures are used in large-span space structures, prestress is usually applied on frame beams or columns to improve their load-bearing capacities and stiffness. Then, prestressed concrete (PC) frame structures come into being. As load-carrying members in PC frame structures bear much more load than those in common RC frames, PC frames will encounter higher collapse risk once local load-carrying members fail in accidental events. Fan et al. [15] experimentally studied the collapse performance of two single-story and two-bay RC frames strengthened with external prestressing tendons, and the calculating formula for ultimate load of RC frames with external prestressing tendons was derived on the basis of the tests. Qian et al. [16] studied the collapse resistance of posttensioned concrete beam-column subassemblages with unbonded posttensioning strands and found that the effective prestress may significantly affect the ultimate deformability and load capacity of the PC frames. To date, limited research works have been done on progressive collapse of PC frame structures. It is necessary to reveal their collapse performance such as collapse mechanisms and failure modes. This paper reports the experimental results of five reduced scaled beam-column frame substructures after a middle-column removal; the influence of span-to-depth ratios and prestress action modes on progressive collapse of PC frame structures was assessed. In addition, a calculation method of dynamic increase factor (DIF) of collapse load for PC frame structures was developed.

2. Experimental Design

2.1. Specimen Design. Five one-fourth reduced scaled one-story and two-bay frame substructures were designed referring to a real RC frame building, and the location of the substructure in the prototype structure is enclosed by dotted lines, as shown in Figure 1. Each substructure comprises two frame beams and three columns named as column A to column C, respectively, where column B was used to simulate the failed middle column due to accidental load. The five specimens was designated as S1 to S5, in which S1 was the sole specimen without prestress; S2, S3, and S4 were prestressed in the frame beams with unbonded prestressing strands (UPSs), while the frame beams of S5 were prestressed with a bonded prestressed strand (BPS). The geometry and reinforcement details of the five substructures are identical besides prestressing strands. S1 is taken as an example to illustrate the details of the specimens, as shown in Figure 2. The primary design parameters of the substructures are listed in Table 1. Figure 3 shows the layout of the prestressing strands in the frame beams of S2 to S5, where l_0 is the location dimension of the strands and taken as 230 mm and 290 mm for S2 and S4 respectively, as well as 260 mm for both S3 and S5. The minimum distance from the centerlines of the strands to the outside surfaces of the frame beams was 35 mm both in positive and negative moment regions. Longitudinal reinforcing bars (LRBs) in all the columns were welded with steel plates embedded in the column ends. Four threaded rods were embedded in each frame beam stub to connect with the A-shaped reaction steel frame. The nominal diameter of the posttensioned strands is 9.5 mm. The initial effective prestress is about $0.6f_{ptk}$, where f_{ptk} represents the ultimate tensile strength of the prestressing strands. Deformed reinforcing bars of D8, D12, and D16 were used as LRBs and round reinforcing bars of R8 were used as stirrups in the frame beams and columns. The concrete covers for the beams and columns are all 20 mm. The measured mechanical properties of reinforcement and prestressing strands are listed in Table 2. As for concrete, the axial compressive strength and elastic modulus were tested on six prismatic specimens with 150 mm length, 150 mm width, and 300 mm height, and the tensile strength was tested on six cubes of 150 mm. The measured axial compressive strength, elastic modulus, and tensile strength of concrete were 42.1 MPa, 3.77×10^4 MPa, and 3.6 MPa, respectively.

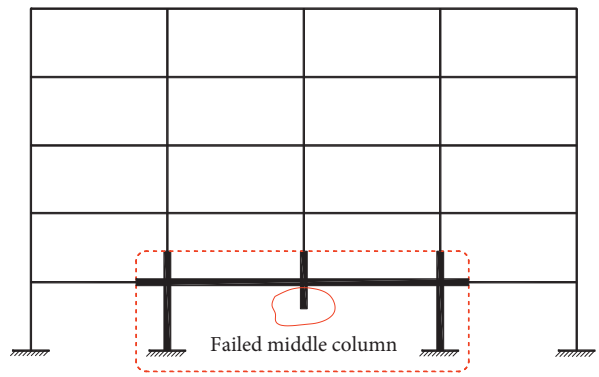

Figure 1: Location of the substructures in the prototype structure.

2.2. Loading Procedure. The loading procedure was divided into two steps for each substructure. Firstly, the test of fast removing the middle column was conducted. During the test, temporary support was set at the bottom of column B in advance and then steel weight was hung on the quartile points of each frame beam to simulate the load transmitted from the adjacent floors, which was taken as 10.0 kN/m^2 according to load design code of China, whereafter, the temporary support was removed rapidly by striking. Dynamic responses of the residual substructures, including acceleration, dynamic displacement, and so on, were recorded. Secondly, static collapse test was carried out by applying vertical monotonic load on the top of column B until the final failure occurred, which will be mainly

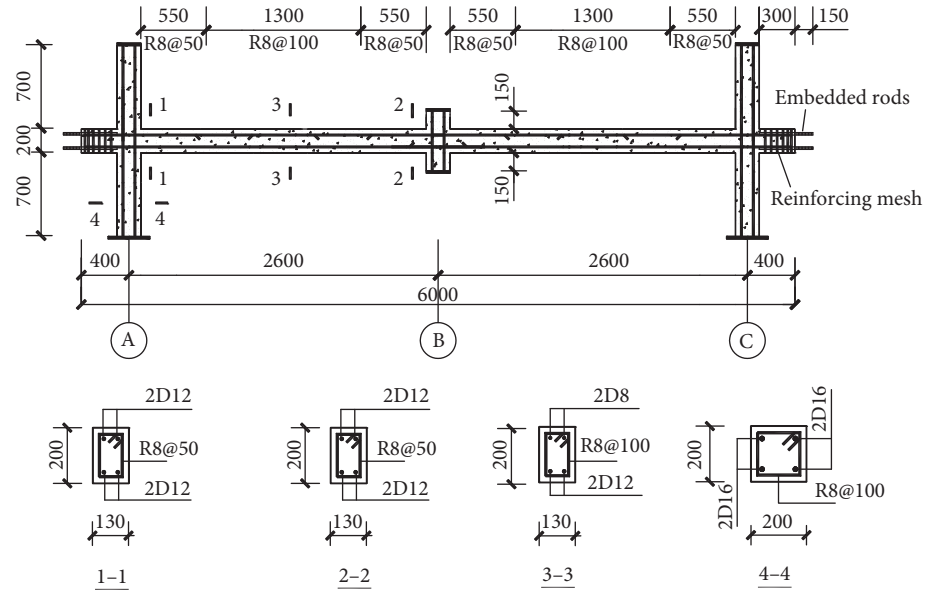

Figure 2: Dimensions and reinforcement of S1.

Table 1: Design parameters of the specimens.

Specimen	Span of frame beam (mm)	Clean span-to-depth ratio of frame beam	Initial effective prestress	Prestress action modes
S1	2600	12.0	N/A	N/A
S2	2300	10.5	0.6 f_{ptk}	Unbonded prestress
S3	2600	12.0	0.6 f_{ptk}	Unbonded prestress
S4	2900	13.5	0.6 f_{ptk}	Unbonded prestress
S5	2600	12.0	0.6 f_{ptk}	Bonded prestress

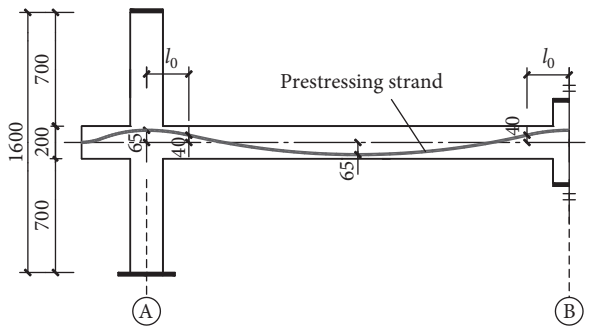

Figure 3: Layout of the prestressing strand.

discussed in this paper. Note that suspension weight on the frame beams was taken away from the beams during the static collapse tests.

Figure 4 illustrates the details of the specimen assembly in the static collapse tests. Vertical load was applied on column B through a steel column by a hydraulic jack with a stroke of 700 mm. The steel column passed through a steel box with eight steel rods arranged in the two orthogonal directions, which could prevent the steel column from free rotation. Axial compressive load was applied on the top of the two side columns by hydraulic jacks to simulate the load transferred from the upper columns, and the corresponding axial load ratio was approximately 0.5. The two side columns' feet were connected with steel girders by bolts, and the steel girders were fixed on the strong test bed using ground anchors. Four threaded rods were embedded in each frame beam stub that extended outward from the side column, through which the frame beams connected with A-shaped reaction frames. The distance from the constrained positions of the upper parts of the two side columns, being approximately the inflection points of the upper columns, to the top surfaces of the frame beams was about 450 mm.

2.3. Measuring Instruments. Displacement meters were arranged along the beams to measure the vertical displacement, as shown in Figure 4. Monotonic static load applied on the top of column B was measured by a pressure load cell. The horizontal reaction forces acting on the frame beam stub and the upper part of the side column were measured by tension-compression load cells. Strain gauges were mounted on the LRBs at the cross sections 1-1 and 2-2 of the frame beams, as shown in Figure 2.

3. Experimental Observations

In the dynamic collapse tests, a few cracks were observed in the regions of the beam ends for all thesubstructures after the temporary supports were removed. A small amount of residual deformation was observed even after the hung steel weight was taken away from the frame beams at the end of the tests. According to the measured microstrain of LRBs, it

Table 2: Mechanical properties of reinforcement and prestressing strands.

Items	Nominal diameters (mm)	Yield strength (MPa)	Ultimate strength (MPa)	Elastic modulus (MPa)	Elongation (%)
R8	8	371.0	550.2	2.1×10^5	10.8
D8	8	449.2	670.8	1.9×10^5	8.5
D12	12	429.1	583.9	2.0×10^5	12.2
D16	16	539.0	711.4	2.0×10^5	14.3
Prestressing strand	9.5	1812	1926	1.9×10^5	5.5

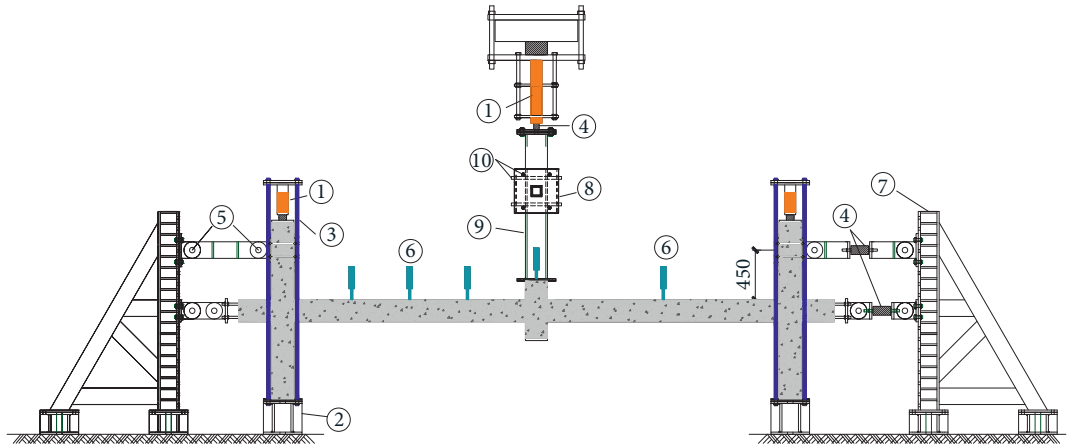

① Hydraulic jack
② Steel girder
③ High-strength screws
④ Load cell
⑤ Hinge joints
⑥ Displacement meter
⑦ A-shaped reaction frame
⑧ Steel box
⑨ Steel column
⑩ Steel rods

Figure 4: Specimen assembly.

was identified that the residual substructures were still in elastic working stage after the middle-column loss. Therefore, the influence of the residual deformation produced in the dynamic collapse tests was neglected in the following discussion of the static collapse test results. The experimental observations of the specimens in the static collapse tests can be summarized as follows:

S1: at the initial loading process, new cracks firstly appeared at the bottom of the beam ends near to the middle column (BENMC) and then appeared at the top of the beam ends near to the side columns (BENSCs). With the increase of vertical displacement, concrete at the beam ends gradually crushed and major cracks finally ran across the whole beam sections. Concrete at the feet of column A and column C cracked at the vertical displacement of 60.1 mm and 120.0 mm, respectively, and locally crushed at the later loading stage. The test ended at the load of 73.7 kN due to severe damage of the beam ends. At that moment, the vertical displacement at column B was about 400 mm. The failure pattern of S1 is shown in Figure 5(a).

S2–S4: specimens S2, S3, and S4 were designed to investigate the influence of span-to-depth ratios of the frame beams on progressive collapse of PC frame structures. Phenomena of the three specimens were similar to that of S1; that is, new cracks firstly appeared at the beam ends and then concrete in the compression zone of the beam ends gradually crushed. Once the posttensioned strands fractured, the collapse resistance of the specimens reduced abruptly. Comparing with S1, cracks on the frame beams of the three specimens were sparser and wider. A few tiny cracks were observed on the outer surfaces of the side columns near to the beam-column joints during the tests. The failure patterns of the three specimens are shown in Figures 5(b)–5(d).

S5: the only difference between S3 and S5 was the prestress action mode, i.e., the frame beams of S5 were prestressed with a BPS. Similar to S3, a series of cracks appeared on the frame beams of S5, while cracks on the beams of S5 were tinier and the main cracks' widths were relatively narrower. The failure pattern of S5 is shown in Figure 5(e).

4. Experimental Results

4.1. Collapse Resistance Capacity. Figure 6 illustrates the relationship between load and vertical displacement at column B. The collapse process could be divided into three stages, that is, the elastic stage, the elastic-plastic stage, and the failure stage. (1) The elastic stage: in this stage, the

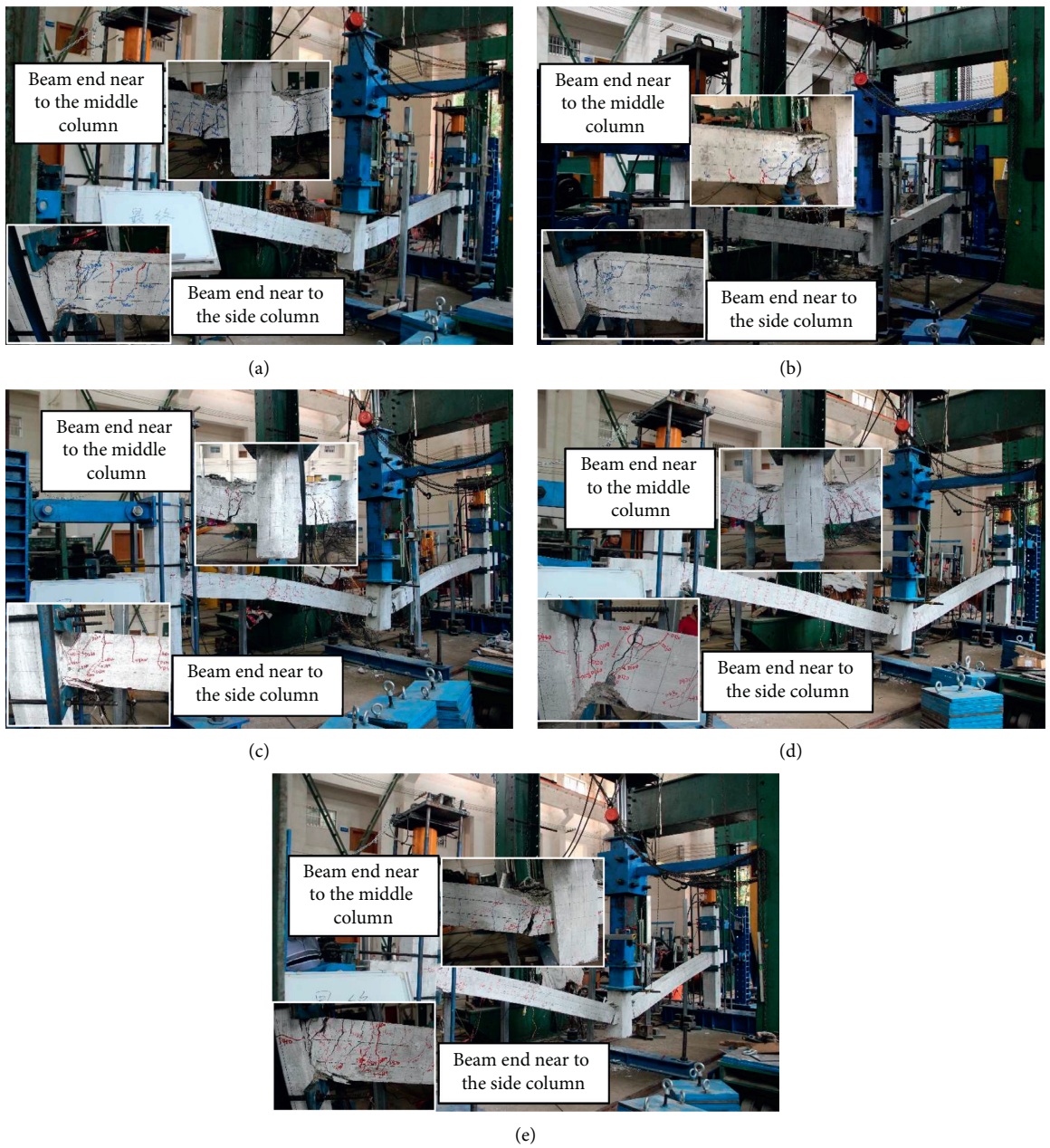

Figure 5: Failure patterns of the specimens. (a) S1. (b) S2. (c) S3. (d) S4. (e) S5.

vertical displacement of the frame beams almost linearly increased with the load applied on column B, but the duration of this stage was relatively short. (2) The elastic-plastic stage: when the applied load kept rising, large deformation and plastic strain produced in the substructures, and then the first peak load appeared. Thereafter, the number of cracks on the beams increased markedly, some cracks at the beam ends propagated from the tensile zone to the compressive zone of the beams, and then the load-bearing capacity of the residual substructures began to decrease. Plastic hinge mechanism finally formed when the LRBs in the BENSCs yielded and eventually vanished after concrete in the regions of plastic hinges crushed. During this process, the load-bearing capacity of the substructures reached the troughs. (3) The failure stage: when the compressive stress of the LRBs in the beam ends changed into tensile stress, it meant the formation of the catenary action. Thereafter, the load-bearing capacity began to ascend again after reaching the trough. The final failure usually occurred when the LRBs or the prestressing strands in the beam ends fractured. The primary experimental results are listed in Table 3. Based on the experimental results, the inherent characteristics of collapse resistance capacity of the substructures are discussed as follows:

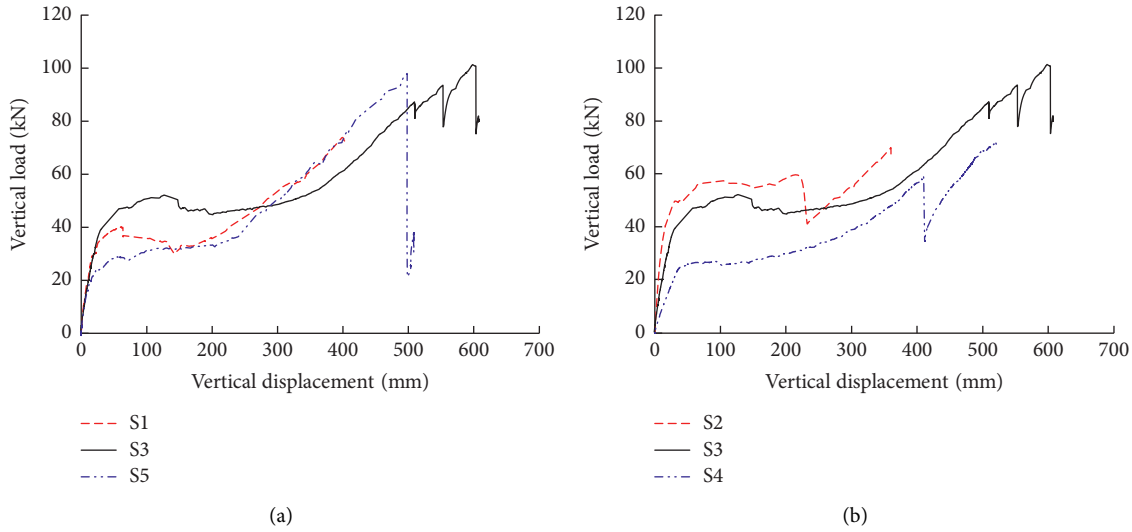

Figure 6: Relationship between vertical load and displacement. (a) Influence of prestress. (b) Influence of span-to-depth ratios of the frame beams.

Table 3: Experimental results.

Specimen ID	The yield load of frame beams P_y (kN)	The first peak load P_P (kN)	Load at the beginning of catenary action P_t (kN)	Vertical displacement at P_y (mm)	Vertical displacement at P_P (mm)	Vertical displacement at P_t (mm)
S1	33.4	40.1	30.1	25.0	61.7	142.0
S2	43.6	57.4	41.1	21.1	104.7	232.2
S3	36.4	52.1	45.3	25.4	127.0	212.7
S4	22.3	N/A	N/A	32.4	N/A	N/A
S5	24.2	N/A	N/A	29.7	N/A	N/A

N/A represents the unavailability of data.

(1) S1, S3, and S5 were designed to investigate the influence of prestress on progressive collapse of PC frame structures. Figure 6(a) shows the load-versus-vertical displacement curves of the three substructures. Comparison showed that the first peak load of S3 was 1.30 times that of S1. Although the first peak load of S5 was inconspicuous, it was obviously the lowest one. Ranking of the first peak loads in descending order is S3, S1, and S5 in turn. It can be seen that the first peak load of S1 was not as low as expected. After the first peak load appeared, the load-bearing capacity of S3 kept stable for a long period, while that of S5 grew slowly instead of decreasing. Compared with S3 and S5, S1 possesses the lowest collapse resistance at the final failure; it proves that prestress is helpful to improve the ultimate collapse resistance of RC frame structures.

(2) According to Figure 6(b), ranking of the first peak loads for S2 to S4 in descending order is S2, S3, and S4. Before the prestressing strands fractured, the bearing capacity of the specimens maintained an upward trend. Fracture of the prestressing strands usually led to abrupt decrease of the load-bearing capacity. In sum, the frame substructures with smaller span-to-depth ratio have higher initial stiffness, and the ultimate deformability of the PC substructures is tightly connected with the failure of the prestressing strands.

4.2. Horizontal Reaction Forces. Figure 7 depicts the relationship between horizontal reaction forces and vertical displacement at the failed middle column, where N_c and N_b represent the horizontal reaction forces acting on the frame beam ends and the upper parts of the side columns, respectively. It shows that the upper parts of the side columns and the frame beam ends were mainly subjected to horizontal pull in the later loading stage. The horizontal reaction forces acting on the beam ends of S2 were firstly pressure and then pull; they indicated that the compressive arch action was more obvious for the substructure with smaller span to depth ratio. It can be seen that the structural members adjacent to the failed columns could provide lateral restraints, which contributes to improving the collapse resistance capacity of the frame structures. On the other hand, the adjacent columns should possess enough shear capacity; otherwise, the horizontal progressive collapse of the residual structures perhaps occurs due to poor horizontal load-bearing capacity of the columns near to the failed column.

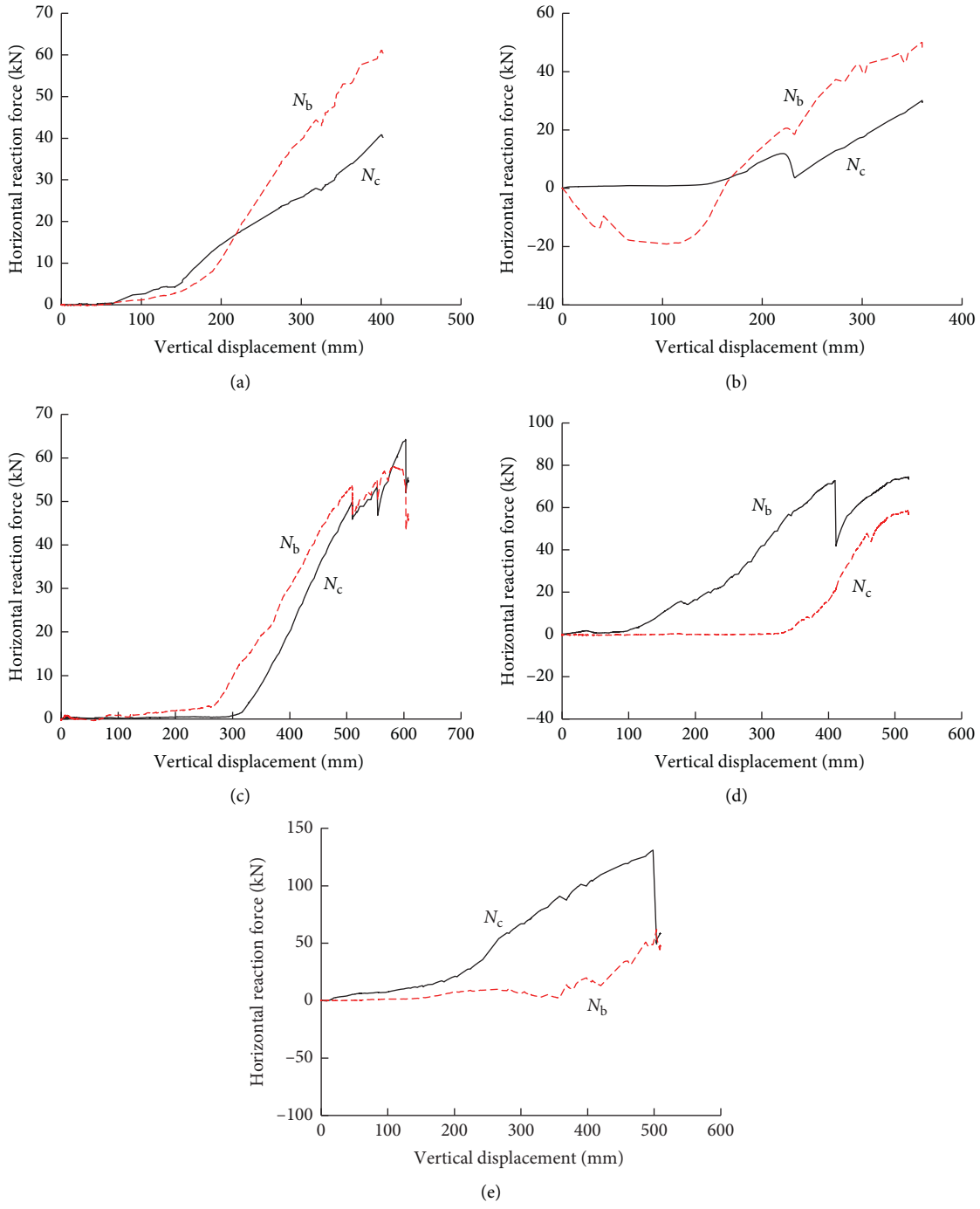

Figure 7: Horizontal reaction forces versus vertical displacement curves (a) S1. (b) S2. (c) S3. (d) S4. (e) S5.

4.3. Microstrain of Longitudinal Reinforcement in the Frame Beams. Strain gauges were mounted on the LRBs to monitor the development of microstrain. The relationship between strain of LRBs at the specified beam sections (sections 1-1 and 2-2) and vertical displacement at column B is shown in Figure 8. The following can be found. (1) The top reinforcement in section 1-1 and bottom reinforcement in section 2-2 sustained tensile stress during the whole tests, while the bottom reinforcement in section 1-1 and top reinforcement in section 2-2 sustained compressive stress at first, which gradually changed into tensile stress with the increase of vertical displacement. The turning points from compressive stress to tensile stress for the LRBs meant the beginning of catenary action. (2) The LRBs in the BENSCs usually yielded earlier than those in the BENMCs; it meant the plastic hinges firstly formed in the beam ends far away from the failed middle columns.

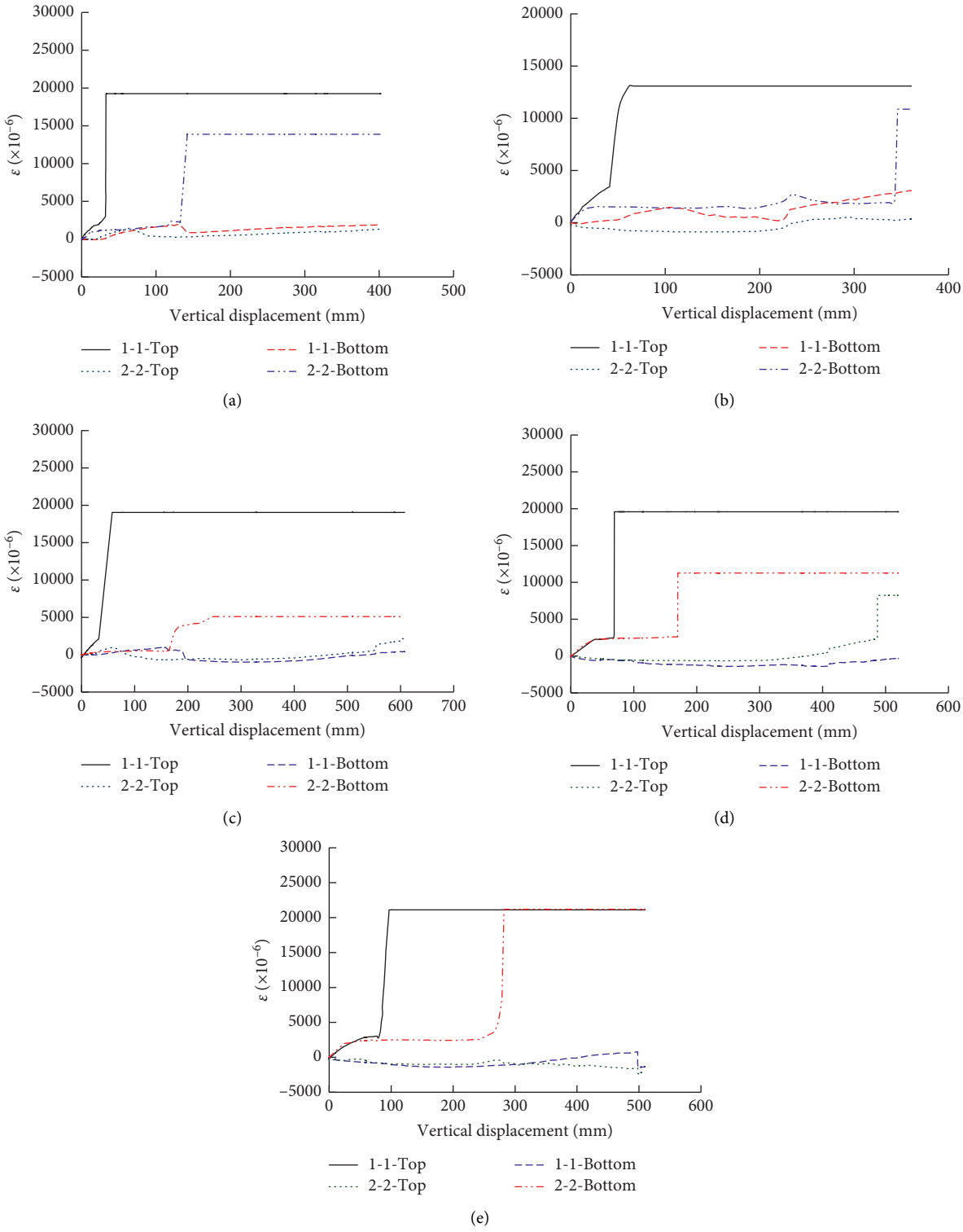

Figure 8: Strain of LRBs versus vertical displacement curves (a) S1. (b) S2. (c) S3. (d) S4. (e) S5.

4.4. Tensile Force Increment of the Prestressing Strands. For S2 to S4, tensile force increment of the UPSs was measured. The curves of the tensile force increment of the UPSs versus vertical displacement of column B are illustrated in Figure 9. It can be seen that the tensile force increment almost linearly increased with the vertical displacement. The UPSs in S2 and S4 finally fractured in the tests, which did not happen on S3. Based on the experimental results, it can be found that the load-bearing capacity of the residual frame substructures decreased immediately once UPSs fractured. Therefore, prestress plays an important role in maintaining the collapse

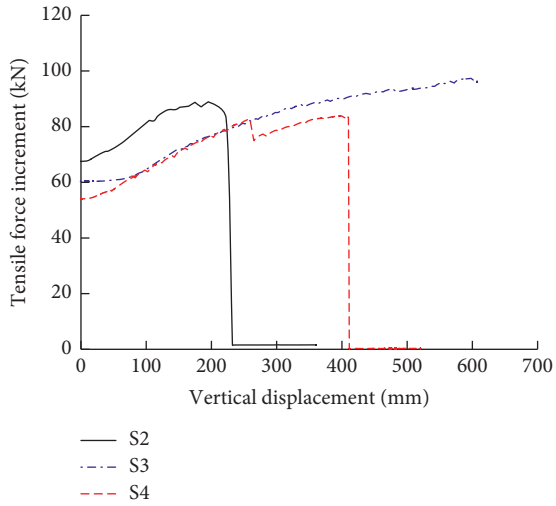

Figure 9: Relationship between tensile force increment and vertical displacement.

resistance of the residual structures in the scenario of a middle-column loss.

5. Discussions

5.1. Mechanical Mechanism against Collapse. Three primary mechanical mechanisms successively formed during the collapse of the residual PC frame substructures. (1) After removing the middle column, the adjacent two frame beams beside the failed middle column in the substructures changed into one-span beam. According to the measured horizontal reaction forces acting on the beam ends, it was concluded that compressive arch action appeared during the initial loading stage. However, judging from the values of the horizontal reaction forces, effect of compressive arch action on the collapse performance of the residual substructures was not as great as expected. (2) With the increase of vertical displacement, LRBs in the beam ends gradually yielded and beam plastic hinges came into being. Generally, beam plastic hinges firstly appeared in the BENSCs and then appeared in the BENMCs. Beam plastic hinge mechanism was the most important working mechanism against structural collapse before sufficient beam plastic hinges formed. (3) Once concrete in the regions of the beam plastic hinges crushed, compressive zone in the beam ends finally disappeared. Thereafter, LRBs in the beam ends only suffered tension and catenary action mechanism began to dominate the collapse resistance of the residual substructures. The comparison between the first peak loads and the ultimate loads shows that the catenary action could significantly improve the collapse resistance of the substructures.

5.2. Overall Deformation. The deformation curves of the frame beams under different load levels after the failure of column are shown in Figure 10, in which the last load level corresponds to the ultimate load at the end of the tests. It can be seen that the deformation of the frame beams beside the failed middle column almost kept linearly increasing at the initial loading stage. In the later loading stage, the growth of vertical displacement of the beams, along the direction from the side column to the middle column, gradually accelerated under the same vertical load. At this time, the deformation curves of the frame beams became nonlinear. The exceptions were the beam segments beside the failed middle column, the displacement growth of which obviously decelerated comparing with the other parts of the beams in some cases. In general, it can approximately regard the vertical deformation at any position of the frame beams as proportional to the vertical displacement of column B under design collapse load.

5.3. Equivalent Dynamic Increase Factor of Collapse Load. To consider the influence of dynamic impact, dynamic increase factors (DIFs) are often used to revise the collapse load when the alternate path method is adopted to analyze collapse resistance of RC frame structures. Although dynamic collapse tests are the most direct approach to obtain accurate DIFs, numerous tests are needed to achieve this purpose, which is costly and time-consuming. Abruzzo et al. [17] presented a calculation method of DIFs based on energy conservation; however, this method was unsuitable for PC frame structures. In accordance with the method provided by Abruzzo, a calculation method of DIFs for PC frame structures is developed as follows:

(1) As the prestressing strands are arranged in parabolic curves, the initial effective prestress of the prestressing strands can be converted into uniform loads that segmentally distributed on frame beams using the load balance method. The equivalent uniform loads $q_i\,(i = 1, \ldots, 5)$ for the PC frame substructures in this paper are shown in Figure 11.

(2) Assume that the vertical displacement at any position of the frame beams is proportional to the vertical displacement, Δ_s, of the failed middle column. In addition, the initial prestress of the prestressing strands is regarded as a type of external force. Then, the work, $W_p(\Delta_s)$, done by the initial prestress during the collapse can be calculated as follows:

$$W_p(\Delta_s) = \sum_{i=1}^{n} \int_0^{l_i} q_i \Delta_i(x)\mathrm{d}x, \quad (i = 1, \ldots, 5), \tag{1}$$

where $\Delta_i(x)$ is the vertical displacement at any position of the frame beams and l_i is the load distribution lengths of the equivalent uniform loads along the frame beams.

(3) Given that the load applied on the top of the failed column is P and the corresponding vertical displacement here is Δ_s. Then, the equivalent dynamic load, $P_{d,\mathrm{eq}}$, of the total external forces is

$$P_{d,\mathrm{eq}} = \frac{W_p(\Delta_s) + \int_0^{\Delta_s} P\Delta\mathrm{d}\Delta}{\Delta_s}. \tag{2}$$

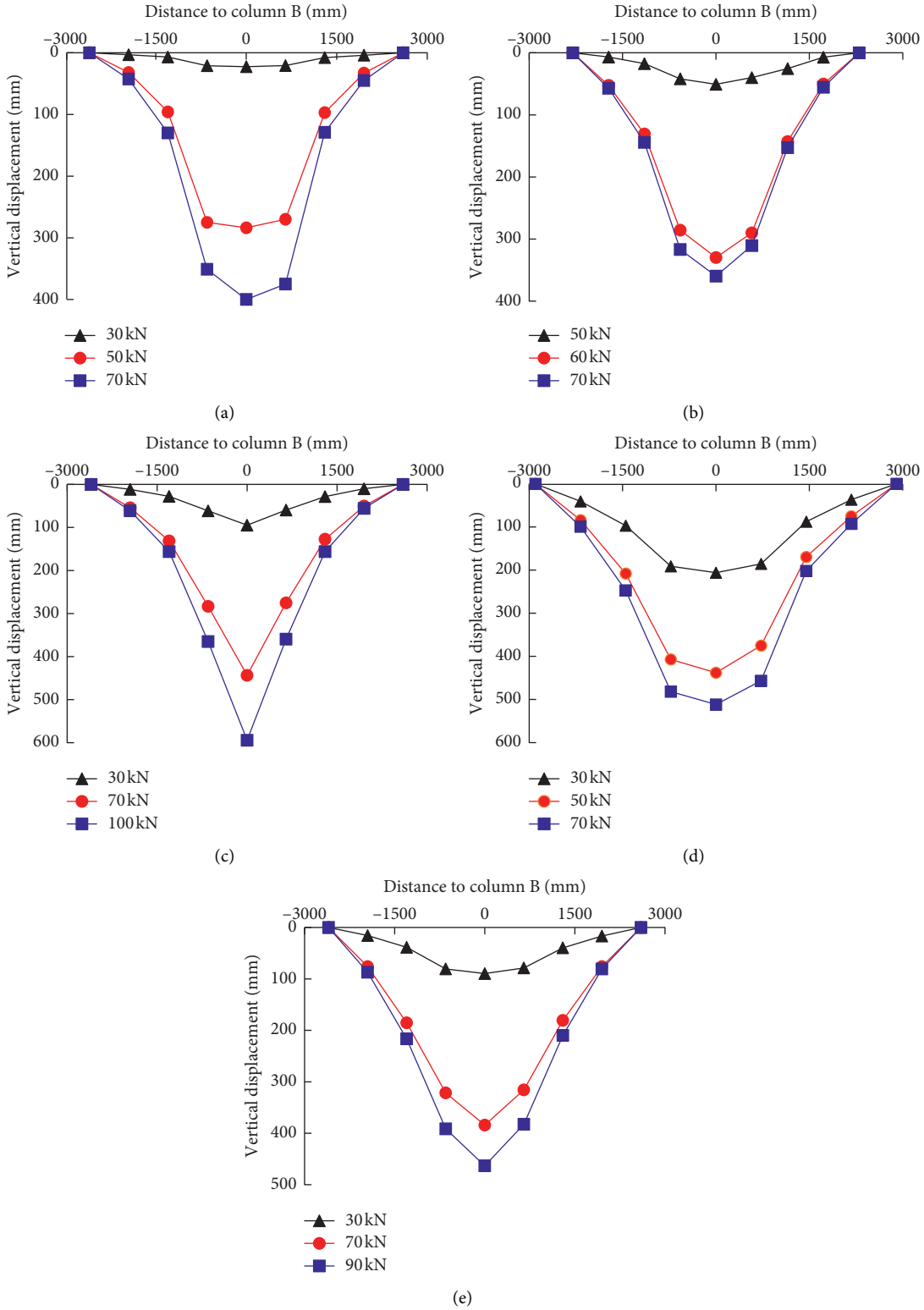

Figure 10: Overall deformation of frame beams. (a) S1. (b) S2. (c) S3. (d) S4. (e) S5.

(4) Order $(W_P(\Delta_s)/\Delta_s) = P_{PP}$, and $(\int_0^{\Delta_s} P\Delta d\Delta)/\Delta_s = P_P$; then equivalent DIF can be defined as the ratio of the total static load to the equivalent dynamic load:

$$\text{DIF} = \frac{P + P_{PP}}{P_P + P_{PP}}. \tag{3}$$

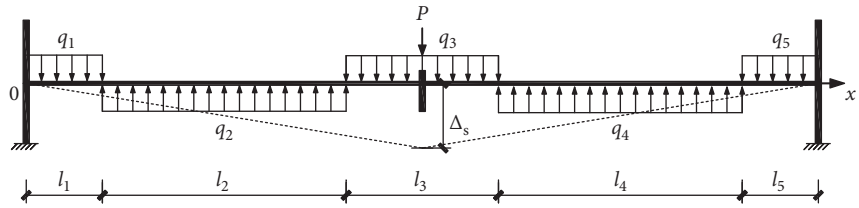

Figure 11: Equivalent uniform loads of the initial prestress.

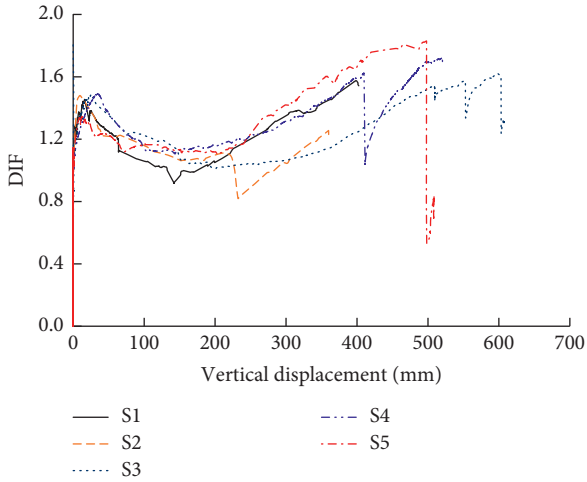

Figure 12: Relationship between DIFs and vertical displacement.

Table 4: DIFs at different loading stages.

Specimen ID	DIF_P	DIF_u
S1	1.46	1.57
S2	1.44	1.24
S3	1.48	1.62
S4	1.49	1.68
S5	1.34	1.83

According to the developed method, the relationship between the equivalent DIFs and the vertical displacement for S1 to S5 was obtained, as shown in Figure 12. It can be seen that DIFs increased rapidly at the initial loading stage and began to decrease after reaching the first peak points. Once the DIFs reduced to the troughs, they began to ascend slowly until the final failure of the substructures. DIF_P and DIF_u are listed in Table 4, which correspond to the first peak points and the last peak points of the curves in Figure 12. Comparison shows that the maximum values of DIF_P and DIF_u are less than 1.49 and 1.83, respectively. It is noted that not all the energy dissipation types are considered in the proposed method; for example, the energy dissipation due to concrete cracking was neglected. This will result in the calculated $P_{d,eq}$ by (2) being greater and consequently cause the obtained DIFs using (3) to become smaller. Therefore, the accuracy of the proposed calculation method of DIFs for PC frame structures still needs to be validated by a series of dynamic collapse tests and analysis.

6. Conclusions

Collapse tests were carried out on five frame substructures, and the following conclusions based on the experiments are drawn:

(1) In the scenario of a middle-column loss, cracks mainly distributed on the frame beam ends. Comparing with the common RC frame substructure, cracks on the beams of PC frame substructures were wider and sparser. LRBs in the BENSCs yielded earlier than those in the BENMCs during the tests.

(2) Three mechanical mechanisms against collapse successively emerged during the collapse procedure of PC frames, namely, compressive arch mechanism, beam plastic hinge mechanism, and catenary action mechanism. Catenary action is the major mechanism to maintain the load-bearing capacity of the residual frame substructures in the later collapse process. Tensile force increment of the unbonded prestressing strands almost linearly increased with the vertical displacement of the failed column, and prestress was proved to be more important to maintain the load-bearing capacity of the PC frame substructures during collapse.

(3) For PC frame substructure with bonded prestress, the vertical displacement of the failed middle column was even greater than that of the common RC frame substructure at the initial loading stage. The PC frame with unbonded prestress possessed the higher initial stiffness and superior ultimate deformability. The ultimate deformability of the PC frame substructures was tightly connected with the failure of the prestressing strands. Taking reasonable design parameters, including span-to-depth ratios of frame beams and prestress action modes, could mitigate the collapse risk of PC frame structures.

(4) Once the middle column fails, the structural members adjacent to the failed columns could provide lateral restraints, and this helps to improve the collapse resistance capacity of the residual structures. Columns adjacent to the failed column should possess enough lateral load-bearing capacity to avoid possible horizontal progressive collapse of the residual structures.

(5) A simplified calculation method of equivalent DIFs for PC frame structures was developed based on energy conservation. In accordance with the

proposed method, it was found that the equivalent DIFs corresponding to the first peak loads and the ultimate failure loads for the PC frame substructures were less than 1.49 and 1.83, respectively. When static collapse analysis is conducted by alternative path method, the method provided in this paper could be used to determine DIFs of collapse load for PC frame structures.

Data Availability

The data included in this study are available from the corresponding author upon request.

Conflicts of Interest

The authors declare that they have no conflicts of interest regarding the publication of this paper.

Acknowledgments

This research was supported by the National Natural Science Foundation of China (grant nos. 51568005 and 51868004), Chinese Postdoctoral Science Foundation Project (no. 43XB3782XB), and High-Level Innovation Team and Outstanding Scholar Plan of Guangxi High Colleges.

References

[1] Y.-P. Su, Y. Tian, and X.-S. Song, "Progressive collapse resistance of axially-restrained frame beams," *ACI Structural Journal*, vol. 106, no. 5, pp. 600–607, 2009.

[2] W.-J. Yi, Q.-F. He, Y. Xiao, and S. K. Kunnath, "Experimental study on progressive collapse-resistant behavior of reinforced concrete frame structures," *ACI Structural Journal*, vol. 105, no. 4, pp. 433–439, 2008.

[3] J. Yu and K.-H. Tan, "Experimental and numerical investigation on progressive collapse resistance of reinforced concrete beam column sub-assemblages," *Engineering Structures*, vol. 55, no. 4, pp. 90–106, 2013.

[4] K. Qian and B. Li, "Slab effects on response of reinforced concrete substructures after loss of corner column," *ACI Structural Journal*, vol. 109, no. 6, pp. 845–855, 2012.

[5] H. Helmy, H. Salem, and S. Mourad, "Progressive collapse assessment of framed reinforced concrete structures according to UFC guidelines for alternative path method," *Engineering Structures*, vol. 42, pp. 127–141, 2012.

[6] K. Qian and B. Li, "Dynamic performance of RC beam-column substructures under the scenario of the loss of a corner column-experimental results," *Engineering Structures*, vol. 42, pp. 154–167, 2012.

[7] M. Sasani, "Response of a reinforced concrete infilled-frame structure to removal of two adjacent columns," *Engineering Structures*, vol. 30, no. 9, pp. 2478–2491, 2008.

[8] M. Sasani and S. Sagiroglu, "Progressive collapse resistance of hotel san diego," *Journal of Structural Engineering*, vol. 134, no. 3, pp. 478–488, 2008.

[9] J. Hou, L. Song, and H.-H. Liu, "Testing and analysis on progressive collapse-resistance behavior of RC frame substructures under a side column removal scenario," *Journal of Performance of Constructed Facilities*, vol. 30, no. 5, Article ID 04016022, 2016.

[10] G. Kaewkulchai and E. B. Williamson, "Beam element formulation and solution procedure for dynamic progressive collapse analysis," *Computers & Structures*, vol. 82, no. 7-8, pp. 639–651, 2004.

[11] S. Amiri, H. Saffari, and J. Mashhadi, "Assessment of dynamic increase factor for progressive collapse analysis of RC structures," *Engineering Failure Analysis*, vol. 84, pp. 300–310, 2018.

[12] H. M. Elsanadedy, T. H. Almusallam, Y. A. Al-Salloum, and H. Abbas, "Investigation of precast RC beam-column assemblies under column-loss scenario," *Construction and Building Materials*, vol. 142, pp. 552–571, 2017.

[13] S.-B. Kang and K.-H. Tan, "Robustness assessment of exterior precast concrete frames under column removal scenarios," *Journal of Structural Engineering*, vol. 142, no. 12, Article ID 04016131, 2016.

[14] S.-B. Kang and K.-H. Tan, "Progressive collapse resistance of precast concrete frames with discontinuous reinforcement in the joint," *Journal of Structural Engineering*, vol. 143, no. 9, Article ID 04017090, 2017.

[15] Y.-L. Fan, J. Wang, and H.-L. Wang, "Experimental study on collapse performance of one-story reinforced concrete frames using external prestressing tendons," *Journal of Central South University*, vol. 49, no. 5, pp. 1244–1253, 2018.

[16] K. Qian, Y. Liu, T. Yang, and B. Li, "Progressive collapse resistance of posttensioned concrete beam-column subassemblages with unbonded posttensioning strands," *Journal of Structural Engineering*, vol. 144, no. 1, Article ID 04017182, 2018.

[17] J. Abruzzo, A. Matta, and G. Panariello, "Study of mitigation strategies for progressive collapse of a reinforced concrete commercial building," *Journal of Performance of Constructed Facilities*, vol. 20, no. 4, pp. 384–390, 2006.